



LAWRENCE
LIVERMORE
NATIONAL
LABORATORY

Nanofluidic Transport Through Isolated Carbon Nanotube Channels: Advances, Controversies, and Challenges

S. Guo, E. Meshot, T. Kuykendall, S. Cabrini, F. Fornasiero

January 22, 2015

Advanced Materials

Disclaimer

This document was prepared as an account of work sponsored by an agency of the United States government. Neither the United States government nor Lawrence Livermore National Security, LLC, nor any of their employees makes any warranty, expressed or implied, or assumes any legal liability or responsibility for the accuracy, completeness, or usefulness of any information, apparatus, product, or process disclosed, or represents that its use would not infringe privately owned rights. Reference herein to any specific commercial product, process, or service by trade name, trademark, manufacturer, or otherwise does not necessarily constitute or imply its endorsement, recommendation, or favoring by the United States government or Lawrence Livermore National Security, LLC. The views and opinions of authors expressed herein do not necessarily state or reflect those of the United States government or Lawrence Livermore National Security, LLC, and shall not be used for advertising or product endorsement purposes.

DOI: 10.1002/ adma.201500372

Article type: Research News

Title: Nanofluidic Transport Through Isolated Carbon Nanotube Channels: Advances, Controversies, and Challenges

*Shirui Guo, Eric R. Meshot, Tevye Kuykendall, Stefano Cabrini, and Francesco Fornasiero**

Dr. S. Guo, Dr. E. R. Meshot, Dr. F. Fornasiero

7000 East Ave. Lawrence Livermore National Laboratory, Livermore, CA, 94550

E-mail: fornasio1@llnl.gov

Dr. T. Kuykendall, Dr. S. Cabrini

67 Cyclotron Rd, The Molecular Foundry, Lawrence Berkeley National Laboratory, Berkeley, CA 94720

Keywords: nanofluidics, single carbon nanotube, anomalous transport behavior, ionic conductance, single molecule translocation

Owing to their simple chemistry and structure, controllable geometry, and a plethora of unusual yet exciting transport properties, carbon nanotubes (CNTs) have emerged as exceptional channels for fundamental nanofluidic studies as well as building blocks for future fluidic devices that could outperform current technology in many applications. Leveraging the unique fluidic properties of CNTs in advanced systems requires a full understanding of their physical origin. Recent advancements in nanofabrication technology enable building nanofluidic devices with a single, nanometer-wide CNT as a fluidic pathway. These novel platforms with isolated CNT nanochannels offer distinct advantages for establishing quantitative structure-transport correlations compared to membranes containing many CNT pores. In addition, they are promising components for single-molecule sensors as well as for building nanotube-based circuits wherein fluidics and electronics could be coupled. With such advanced device architecture, molecular and ionic transport could be manipulated with vastly enhanced control for applications in sensing, separation, detection, and therapeutic delivery. This Research News article highlights recent achievements in fabricating isolated-CNT nanofluidic platforms, along with the most significant findings each platform enables for

water, ion, and molecular transport. This review also discusses the implications of these findings and remaining open questions on the exceptional fluidic properties of CNTs.

1. Introduction

Fluid flow through nanoscale conduits is important in a variety of biological processes and technological applications, including cell homeostasis and nerve signaling, sensing, energy storage and conversion, physical and chemical separations, and water desalination.^[1] When fluids are confined in nanoscale structures approaching the fluid physical length scale (e.g. slip length, Debye length, and molecular dimension), novel physical phenomena are often observed, many of which remain to be elucidated to enable their future exploitation in advanced devices.^[2] Among nanoporous materials, CNTs have recently emerged as ideal conduits for fundamental nanofluidic research due to their simple, hollow geometry as well as additional unique features detailed below. Furthermore, they are promising building blocks for next-generation fluidic devices that could outperform current technologies in many applications because of their outstanding fluidic^[3-5] as well as mechanical, electronic, optical, and thermal properties.^[6]

A single-wall carbon nanotube (SWNT) is an atomically thin, graphene sheet (conceptually) rolled up to form a seamless, hollow cylinder and, thus, provides an exciting system to test classical theories of fluid flow at the nanoscale.^[7] The diameter of CNTs can be synthetically tuned from the size of a small molecule to tens of nanometers, and their length can be controlled on the sub-micron to millimeter scale. The walls of CNTs are graphitic, and thus the internal surfaces of CNT nanopores are inherently hydrophobic and molecularly smooth. CNTs also maintain their chemical and structural uniformity along their entire length, which is an important advantage considering the typical surface roughness and heterogeneity of other nanopores.^[8, 9] In addition, well-defined sites for chemical functionalization at the entrance of a CNT nanochannel can be easily targeted to create selective gates for molecular transport without affecting the interior walls. Given their simple structure and chemistry, CNTs are readily simulated with high accuracy and, as one of the few solid-state nanochannels providing this advantage, they have been widely used as model systems to understand fluid flow under spatial confinement. Finally, CNTs share several structural motifs with biological nanochannels, including a narrow hydrophobic core, local selective gates, and a structure that is known with atomistic details. Thus, employing CNTs as simple biomimetic pores could greatly help the understanding of functional behavior in inherently complex biological pores.^[10, 11]

The most intriguing and surprising fluidic properties of CNTs emerge when their diameter is smaller than 10 nm. These include: (a) spontaneous wetting of the hydrophobic CNT interior by aqueous solutions; (b) selective transport of ions and molecules when the CNT opening is functionalized;^[10, 12] and, most importantly, (c) ultra-rapid gas,^[13, 14] water,^[13, 15, 16] and proton^[17] permeation rates that often surpass those of other similarly-sized nanopores by orders of magnitude. Fast flow in CNTs was first predicted by molecular dynamics simulations^[14, 17-20] and then validated by membranes fabricated with billions of vertically aligned CNTs as the only conductive pores^[13, 15] under a static or osmotic pressure driving force. The origin of fast flow in CNTs is attributed to both the ordering of fluids under spatial confinement and the molecularly smooth and hydrophobic walls that promote fluid slip.^[16, 19-21] Molecular dynamics calculations were also able to predict spontaneous water wetting^[19, 22] and structuring inside a CNT^[7, 23] – results which were validated later using a variety of experimental techniques.^[3] Surprisingly, molecular dynamics simulations suggested that complex molecules, such as single-stranded DNA (ssDNA)^[24] and RNA,^[25] can translocate through narrow diameter SWNTs. The fact that water, ions, and biologically relevant molecules can be transported through the inner volume of CNTs at rates that approach the efficiency of complex biological pores further justifies the use of CNTs as exceptional synthetic mimics of biological nanochannels.^[11]

These exciting molecular dynamics results and early experimental findings with CNT membranes paved the way for many potential applications that exploit ultra-rapid and selective transport in CNTs. For example, CNT fluidic channels could potentially function as perfect nano-syringe and drug-delivery conduits,^[26] single-molecule sensors, nanoscale reactors for gas- and solution-based chemistry,^[27] building blocks for energy-efficient desalination membranes or protein separation systems,^[28] energy storage and generation,^[5, 29] ultra-breathable fabrics, etc. In addition, owing to their excellent electronic properties and large surface-to-volume ratio, CNTs may offer new routes of electrical detection, trapping, and manipulation of charged molecules by marrying nanoelectronics and nanofluidics in a new class of nanotube-based circuits.^[9, 30]

This remarkable potential for a wide range of fluidic applications motivated a very recent wave of new experimental studies to elucidate the physics of the unique nanofluidic phenomena in CNTs. These new studies, which are the focus of this review, adopt fluidic platforms with a single conductive CNT channel. Fluidic measurements performed on an individual SWNT are expected to provide a quantum-leap advancement of the nanofluidic

field by unraveling detailed structure-property correlations that otherwise cannot be assessed with multi-pore CNT membranes. Indeed, single-CNT platforms provide distinct advantages with respect to membranes. First, a single nanochannel platform avoids complications due to polydispersity in pore size, and it enables a quantitative interpretation of the observed transport rates as a function of the geometrical and structural properties of the pore. Second, the impact of SWNT electronic type (metallic or semiconducting) on fluidic properties can be investigated, and the unique electronic characteristics of SWNTs can be exploited in advanced nanoelectronic/nanofluidic devices. Third, stochastic events and time-dependent properties, such as gating, are easily isolated when only a single fluidic channel is conducting, whereas this information is lost in conventional CNT membranes because the measured transport behavior is an average across billions of pores.^[8] Finally, being able to isolate and address an individual CNT nanochannel offers great opportunities for label-free single-molecule detection and unprecedented control of ionic and molecular transport.

Therefore, developing advanced fabrication techniques for making well-defined, robust single-CNT platforms with dimensions on the nanometer scale is crucial for both fundamental studies and applications, yet this remains challenging. In particular, strategies must be designed not only to address transport through a single CNT channel, but also to ensure that fluid flow is indeed through the nanotube core, rather than through defects in the surrounding barrier matrix. The best evidence of transport through a single, isolated nanopore is the observation of two-level stochastic pore-blocking by a guest molecule whose size is comparable to the fluidic channel when employing the Coulter method, also known as resistive pulse sensing.^[31] This is a simple technique that enables quantification of both ionic transport and nanometer-sized, single-molecule transport in an isolated nanopore of commensurable diameter without the need of any label.^[32, 33] In essence, the technique relies on recording the ionic current across a single nanochannel, which connects two electrolyte solutions, under an applied voltage difference. When molecules with a size on the order of the channel diameter are added to one of the electrolyte solutions, their passage through the pore induces a measurable transient blockade of the base ionic current with an amplitude proportional to the molecular size (typically greater than tens of pA), a frequency that correlates with analyte concentration, and a dwell time that contains information on the velocity of molecule translocation across the nanochannel. The current blockade reflects the reduced number of current-carrying ions inside the pore, which is caused by the displacement of an amount of the electrolyte solution equivalent to the volume of the translocating molecule. Thus, clear signatures of fluid transport through a single channel are transient

current blockades with only two states: 1) the open-pore baseline current and 2) the current level of the blocked pore. Absence of current blockades could indicate that alternative transport pathways with width much larger than the probe molecules dominate the current signal, while the presence of multiple current levels is often a signature of several open channels with diameters commensurate with the probe molecule.

In this review, we summarize successful nanofluidic platforms based on isolated CNT channels and emphasize the most significant findings each platform enabled. We also discuss a wealth of unexpected physical phenomena and the controversies remaining in the field, with dedicated subsections for water, ionic, and molecular transport. Finally, our future outlook highlights the need to resolve several open questions and traces the most promising directions for the field of CNT nanofluidics.

2. Single CNT Nanofluidic Platforms

Several approaches demonstrated fluidic platforms where an isolated CNT provides the conductive pathway across an impermeable matrix. Fabricated devices differed greatly in the material used as an impermeable barrier, CNT length and orientation, CNT type and source, ability to characterize SWNT electronic properties, and processes to open CNTs for molecular transport. **Figure 1** collects schematic representations of these platforms and their key features are summarized in **Tables 1-3**. Detailed descriptions are given in the following subsections for solid-state micron-long CNT devices and hybrid systems with ultrashort (<50 nm) SWNTs spanning a lipid bilayer.

The studies reviewed here used various control tests to infer that, in these platforms, transport is indeed through a single CNT and/or to exclude alternative pathways, and the readers are referred to the cited literature for details. However, not all platforms showed the expected two-state Coulter response (the most convincing evidence of single pore transport).^[32] In some studies, the Coulter test was not performed, while in other studies the addition of a nanometer-sized probe molecule induced an unusual transient current *increase* instead of a blockade. While not sufficient evidence of single pore transport, a transient current enhancement may occur when the counter-ions accompanying a translocating charged molecule dominate over the steric blockage effect, thus resulting in a greater number of current-carrying ions inside the pore.^[34, 35, 36] In **Tables 1-3**, for each fluidic platform discussed in this review, we indicate if the Coulter test was performed and what probe molecules were used. We also specify if transient current blockades or unusual increases

(spikes) were observed upon addition of a nanometer-size molecule in one of the electrolyte chambers.

2.1. Solid State Platforms

2.1.1. Vertical CNT Channels

The first successful fluidic device fabricated from an individual, isolated CNT was reported by Crooks et al.^[8, 37] in 2000. They formed 1- μm thick membranes with a single, 80-150 nm wide CNT pore by microtoming an epoxy block with an embedded $\sim 400\text{-}\mu\text{m}$ -long multi-wall carbon nanotube (MWNT). The film was then mounted onto a micron-sized hole formed in a freestanding membrane support^[8, 38] and employed for single-channel particle translocation studies with the Coulter-counter technique (**Figure 1a**). The key advantage of this fabrication method is that hundreds of identical pores can be formed from a single MWNT, which allows highly reproducible results. This platform was used for the first quantitative study of mass transport through a single CNT. Because several interdependent transport modes (diffusion, convection, electrophoresis, electroosmosis, etc.) can contribute to the total velocity of a given species, isolating a single contribution is often non-trivial and not always possible with the Coulter method. Crooks' et al.^[8, 32, 39] provided strong evidences that, for these large tubes, electroosmotic flow and effects of wall charges were both negligible. They determined that, in fact, electrically-driven transport arose only from electrophoresis, which enabled a straightforward simultaneous determination of both average and polydispersity of nanoparticle size, concentration, charge, and mobility. Results obtained using this large MWNT pore platform are consistent with conventional expectations for an uncharged cylindrical pore of similar size. Aside from its high reproducibility merit, this fabrication approach has been demonstrated only for $>50\text{-nm}$ wide MWNTs, which excludes the regime of CNT pore sizes ($<10\text{-nm}$) that is most compelling. Thus, in the remaining sections, we turn our attention to small-diameter CNT devices.

2.1.2. Horizontal CNT Channels

Advances in nanofabrication have made it possible to build fluidic devices with a single, horizontal channel constructed from a SWNT. Lindsay's group was the first to develop a solid state platform with this configuration^[40] by coating a horizontal SWNT with a poly(methyl methacrylate) layer (PMMA) and subsequently patterning by electron-beam lithography (EBL) to define two fluid reservoirs and open either end of the SWNT channel to those

reservoirs (**Figure 1b**). These devices each contained one SWNT that was 0.9-4.2 nm in diameter and 2 μm long, and they were used to probe both ionic transport and molecule translocation driven by an external electric field.^[40, 41] Later variations of this platform include longer SWNTs and a wider barrier layer (20 μm)^[42-44] of a different material (~20-nm SiO_2 covered by PMMA).^[42, 44] To enable optical detection of translocating dye molecules, in one of these studies the device was supported by a cover glass^[42] rather than by a Si/ SiO_2 chip.^[43, 44] One notable strength of this horizontal platform configuration was that the SWNT nanofluidic channel could also be electrically integrated with an EBL-patterned electrode to gate ionic transport^[44] or with contact electrodes to form a field-effect transistor (FET).^[43, 45] This novel device structure enabled simultaneous investigation of the electronic and fluidic properties of a SWNT. In a study by another team,^[46] an array of three p-type FETs was fabricated on an individual, millimeter-long CNT to measure the flow rate of water inside the CNT during spontaneous internal wetting (**Figure 1c**). Contrary to all other platforms in this review, the horizontal CNT devices described above did not show two-state blockades during molecule translocations, and used other control tests to support the claim of transport through a single nanotube.

Strano's group^[47-49] used conventional photolithography to pattern an epoxy structure that was then bonded to an Si/ SiO_2 wafer, which hosted a sparse array of horizontally aligned SWNTs grown in place by chemical vapor deposition (CVD) (**Figure 1d**). In these devices, the CNT fluidic channel had diameters of 1.3-2.3 nm and lengths in the range of 500- μm . These ultralong (>100 μm) CNT channels were employed to investigate transport behavior of both ions and protons inside CNTs.

2.2. Hybrid Platforms

2.2.1. CNT Channels Embedded in Lipid Bilayers

More recently, two groups reported a novel CNT-lipid hybrid membrane platform consisting of ultrashort, 1-2 nm diameter CNTs that span the thickness of a lipid bilayer (~4-5 nm thick) (**Figure 1e**).^[50, 51] Liu et al.^[50] controlled a micro-injection probe with a micromanipulator to directly insert oxidized CNTs into a lipid bilayer membrane. The oxidation step was used to aid cutting long SWNT down to 5-10 nm fragments. However, this step also produced defects in the CNT wall as evidenced by a low-intensity ratio of the graphitic (G) and defective (D) Raman bands. Geng et al.^[51] exploited the spontaneous incorporation of ~10-nm-long SWNTs into a lipid bilayer to form a single (or a few) conductive pore(s). The short

SWNT fragments were created by a sonication-assisted cutting method that minimized damage to the CNT walls (high G/D~8) and, thus, the possible influence of structural and chemical defects on fluid flow behavior. Notably, Geng et al.^[51] demonstrated that these short CNTs spontaneously incorporated into live cell membranes as well, and recorded their ionic conductance in the cell with patch-clamp measurements. Both CNT-lipid hybrid platforms were primarily employed to investigate ssDNA translocation driven by electrophoresis.

Among these single-CNT nanofluidic devices, the hybrid platform by Geng et al.^[51] was built at Molecular Foundry, while a new solid-state platform is currently being developed at this institution to address open questions in both ionic and molecular transport through CNT channels.^[52]

3. Fluid Transport in Isolated CNTs

3.1. Water Transport

3.1.1. Advances

The behavior of water confined in nonpolar nanopores is critical in many biological and technological processes (protein folding, gating in biological channels, membrane distillation, etc.), yet not fully understood. Its complexity and importance motivated extensive molecular dynamics investigation of water wetting and transport in (hydrophobic) CNTs.^[7] These computational studies first revealed that water spontaneously fills small-diameter SWNTs and that transport is rapid and nearly frictionless through their cores.^[16, 19, 21, 22] While several research groups have experimentally measured the magnitude of pressure-driven water flow rate using membranes with large numbers of open CNTs,^[13, 15] experimental studies aiming to elucidate and accurately quantify water motion within a single CNT are rare. Qin *et al.* fabricated an array of three parallel FETs along the length of a millimeter-long SWNT in order to measure the water velocity during spontaneous internal wetting.^[46] The water velocity could be calculated from the distance between FETs and the arrival time of the water front, which was signaled by an increase in FET resistance. The recorded water-flow velocities fell in the range of 46-928 $\mu\text{m/s}$ for CNTs of 0.81-1.59 nm diameter, increasing for smaller CNT diameters. The calculated water-flow enhancement with respect to predictions of continuum Hagen-Poiseuille theory was large ($10\text{-}10^3$) and decayed non-monotonically with CNT diameter. The existence of a discontinuity in the flow enhancement suggested a transition from continuum to sub-continuum flow at diameters less than 1-nm, which is consistent with theoretical predictions.^[53]

3.1.2. Open Questions

While both simulations^[16, 20, 21, 54, 55] and experiments^[13, 15] with CNT membranes demonstrated enormous water flow velocities up to 4-5 orders of magnitude faster than predicted by continuum hydrodynamic theory of Hagen-Poiseuille, large uncertainties remain in the magnitude of this enhancement factor and corresponding slip lengths.^[56] These large deviations in the experimental results are most likely the consequence of challenges associated with accurately quantifying the number of conducting CNTs, their size distribution, and other structural properties of the CNT membrane. To eliminate such uncertainties, Qin *et al.*^[46] has directly measured water velocity in a single, well-defined CNT, whose structure was readily quantifiable. In agreement with simulation predictions,^[53-55] their work suggests that the water-flow enhancement with respect to Hagen-Poiseuille law is less than 1000 and it sits at the lower end of experimental results that used membranes with 1-2 nm CNT pores (see **Table 1**).^[13] However, the estimate by Qin *et al.* relies on molecular dynamics simulations to calculate the driving force for transport rather than experimentally measuring it.^[46] Therefore, these results are not conclusive, and an accurate measurement of flow enhancement and its dependence on CNT pore dimension is still needed.

3.2. Ion Transport Driven by Electric Field

3.2.1. Advances

Understanding ionic transport inside graphitic channels is crucial for many applications including sensing, energy storage/generation, separation, and lab-on-a-chip devices. The novel platforms discussed in Section 2 revealed several unexpected ionic transport phenomena and the corresponding key results are described below and summarized in **Table 2**.

Using the horizontal CNT platform with an integrated gate electrode of Reference ^[44], Lindsay's group recorded giant ionic conductances (G), up to 44 nS at 1 M KCl^[44] through a 20- μm long SWNT, which is two orders of magnitude larger than predicted from the bulk resistivity of the electrolyte.^[44] They coupled molecular dynamics and continuum calculations to show that this enhancement in conductance is the result of giant electroosmotic flow inside SWNTs, which was further supported by the fact that their devices preferentially carried a negative charge and transported cations. Interestingly, when the platform with 2- μm long SWNT and PMMA barrier layer was employed,^[40] these high currents were observed more

frequently for metallic tubes compared to semiconducting ones, suggesting that the SWNT electronic type may influence fluid flow behavior. Surprisingly, instead of the expected linear relationship at high salt concentration,^[2] the ionic conductance showed a power-law dependence on KCl concentration (*i.e.*, $G \sim c^n$) up to 2 M.^[40, 42, 44] This result was consistent across all platforms developed by Lindsay's group regardless of the device materials parameters,^[40, 42, 44] and this dependence was claimed to be unique to small-diameter SWNTs.^[44] The exponent n , that determines that shape of the curve, was found to be sensitive to the total charge on the SWNT (and/or its immediate environment) as well as the barrier material surrounding the nanotube,^[44] which suggests that the barrier film chemistry may be "seen" by the molecules in the channel through the atomically-thin graphitic wall of a SWNT. For example, a narrow range of n values ($\sim 0.3-0.4$) was found for devices with PMMA barriers, whereas this range was much larger for SiO₂ barriers. Finally, the effect of solution pH was studied with the platform containing 2- μm long SWNT and a PMMA barrier layer.^[40] A reduction in current at low solution pH suggested that negatively charged carboxylic groups at the CNT pore opening played a role in modulating electroosmotic flow and the overall conductance inside the CNT. This also meant that proton transport did not contribute significantly to the giant ionic conductance.^[40]

In contrast to Lindsay's finding, Strano's group observed stochastic pore blocking when individual cations partitioned into ultralong CNT nanochannels and obstructed an otherwise stable baseline current dominated by protons.^[49] In these devices, the blocking events occurred above a threshold voltage, and the current blockade amplitude scaled as $\text{K}^+ > \text{Cs}^+ > \text{Na}^+ > \text{Li}^+$, potentially reflecting changes in the hydration shell size from bulk to nanoconfined environments.^[48] Lowering pH and electrolyte concentration caused the magnitude of both the single-channel current and blockade to increase, which supports the claim that protons are the dominant ion conductors. Impressively, proton conductivity was as large as $5 \times 10^2 \text{ S/cm}$ (6.25×10^8 protons/s), thus approaching the transport rates of highly efficient biological pores such as Gramicidin channels.^[49] Li^+ and K^+ cation mobilities ($\sim 10^{-5} \text{ m}^2/\text{Vs}$) calculated from the dwell time of the blockade event were about two orders of magnitude higher than those found in bulk water and comparable to the mobilities calculated by Lindsay's group.^[44] Under specific conditions, the interplay of stochastic pore blocking and diffusion limitation of protons at the CNT pore mouth manifested in highly synchronized blocking events, which lead to resonant current oscillations (**Figure 2a**).^[49] When the pore was unobstructed by cations, the greater-than-bulk proton conductivity resulted simultaneously in rapid proton depletion in the CNT and accumulation of blocking ions at the

CNT entrance, thus favoring cation partitioning into the SWNT. Conversely, a cation blocking the CNT core promoted a rapid increase of proton concentration near the pore entrance, thus establishing the initial conditions for a new oscillatory cycle.

The same platform by Strano's group was also employed to investigate the influence of CNT diameter and electronic type on ionic transport.^[48] Contrary to Lindsay's findings,^[40] no difference between semiconducting and metallic SWNTs was observed, and the magnitude of the current blockade during K^+ ion translocation followed a non-monotonic function of pore diameter in the range 1-2 nm. This is consistent with molecular dynamics predicting that the trend of transport rate versus CNT diameter is discontinuous for narrow CNTs because internal fluids restructure in order to minimize free energy in the presence of severe spatial confinement.^[53]

Giant ionic conductances were also replicated in one of the ultrashort CNT-lipid hybrid platforms. Liu and coworkers^[50] reported a wide range of ionic currents that, depending on electronic type and diameter, were associated with three distinct classes of CNT channels: 1) metallic CNTs generated the largest conductances, approaching 100 nS; 2) 1-2-nm-wide semiconducting CNTs showed intermediate conductances, close to ~10 nS; and 3) <1-nm-wide semiconducting CNTs exhibited the lowest conductance range (~1 nS).^[50] The I-V curves in these hybrid platforms were linear, except for the last class possibly because ion transport through these sub-1-nm diameter SWNTs requires overcoming the energy penalty of partially stripping the ion hydration layer.^[50] No stochastic pore blocking was observed and the ionic current dropped at low pH, thus excluding protons as primary current conductors. The absence of cation-induced blockade events and a similar dependence on solution pH were also found by Geng *et al.*^[51] However, in this work there was no dependence on the CNT electronic type or on the relatively wide distribution of CNT lengths, and in fact, the specific conductance was in the narrow range 0.63 ± 0.12 nS/M, which is comparable to that of an α -haemolysin channel. KCl conductivity inside this ultrashort SWNT had the same order of magnitude of bulk KCl solution and scaled linearly with electrolyte concentration for >0.2M solutions,^[51] rather than according to a power law as found by Lindsay's team.

3.2.2. Controversies and Open Questions

Single-pore conductance measurements have revealed a rich landscape while exploring ionic transport inside small-diameter SWNTs, including exciting and unexpected phenomena such as giant electroosmotic currents and cation-induced stochastic pore blocking. However, several of these observed phenomena were not confirmed among different CNT nanofluidic platforms

and various research groups. For example, a proton-dominated ionic current and stochastic pore blocking by cations were reported only by Strano and coworkers,^[48, 49] whereas other groups show that K^+ and Cl^- are the primary current carriers.^[40, 44, 50, 51] Lindsay's group was the only team so far to show a sub-linear concentration dependence of KCl solution conductance inside a CNT.^[40, 44] The magnitude of the ionic conductance in a SWNT remains entirely an open debate: while the horizontal, solid-state platforms gave ionic conductances 2-3 orders of magnitude larger than those found in bulk electrophoretic transport,^[40, 44, 48, 49] results from one of the hybrid CNT platforms^[51] and CNT membranes^[57] are consistent with bulk electrolyte resistivity or at most a few times larger. Lindsay's group explained the enormous ionic currents inside isolated CNTs with the presence of giant electroosmotic flows.^[40, 44] Their calculations justified a conductance of this magnitude by assuming large slip lengths and large charges on the CNT wall.^[40, 44] However, while large slip is physically realistic, the origin of this high charge density on graphitic carbon remains unclear.

3.3. Molecular Transport Driven by Electric Field

Several research groups recently investigated single-molecule translocation through isolated SWNTs by recording pulses in the ionic current caused by the transit of the molecule through the nanochannel, and demonstrated that both small charged molecules and larger ssDNA can pass through ultrashort, as well as μm -long CNTs. Key findings are summarized in **Table 3**. These exciting experimental discoveries open the door for the application of these channels toward label-free single-molecule detection and targeted delivery of therapeutics.

3.3.1. Advances

ssDNA:

Lindsay and coworkers^[40] were the first to demonstrate electrophoretic transport of ssDNA oligomers through a SWNT (1.5-2-nm wide, 2- μm long) spanning a PMMA barrier layer, and they confirmed the presence of ssDNA at the outlet side of their solid-state device using quantitative polymerase chain reaction (PCR) analysis. Although counterintuitive, considering the hydrophobic nature of CNTs, translocation of these large, charged molecular chains was correctly predicted by simulations.^[24] Surprisingly, Lindsay's team experimentally observed current spikes^[40] during ssDNA translocation through small-diameter SWNTs (**Figure 2c**), whereas larger MWNT channels showed the expected response of current blockades. This strong current increase in narrow CNTs was at first attributed to polarization outside the tube, possibly induced by an asymmetrical current in the SWNT.^[40] However, later molecular

dynamics simulations suggested that, for weakly charged CNTs, an electrical double layer around ssDNA can dominate the charge excess inside the pore and modulate the large CNT electroosmotic flow, thus resulting in current spikes instead of blockades.^[58] Recorded translocation dwell times ranged from 3 to 100 ms for a 60-nucleotide (nt) strand in a 2- μ m-long SWNT, which corresponds to a translocation velocity of 20-666 μ m/s.

More recently, ssDNA translocation events were also observed in CNT-lipid hybrid devices containing similar-diameter, yet ultrashort (\sim 10-nm) SWNTs.^[50, 51] Contrary to Lindsay's finding, the passage of 120-nt^[50] and 81-nt ssDNA^[51] through the SWNT nanochannel caused transient current blockades (**Figure 2c**). In the latter study, the ssDNA translocation time is comparable with that measured for micron-long SWNTs.^[40] In addition to oligonucleotide detection, this hybrid platform enabled selective identification of a modified base (5-hydroxymethylcytosine) in ssDNA thanks to clear signatures in the current blockade signal.^[50] These results and the relatively long ssDNA dwell time suggest the utility of the SWNT nanochannel in advanced platforms for nucleic acid analysis.^[50, 51]

Small Molecules:

Lindsay's group detected transient current modulations when small molecules (molecular weight \sim 500-1000 g/mol) entered μ m-long SWNTs. Test analytes included single nucleotides,^[41] as well as positively (Rhodamine 6G) and negatively charged (Alexa 546) dye molecules.^[42] The nanofluidic platforms used for studying transport of single nucleotides and dyes consisted of a 2- μ m-long SWNTs spanning a PMMA barrier,^[41] and a 20- μ m-long SWNT spanning a SiO₂/PMMA layer, respectively.^[42] The use of fluorescence dye enabled simultaneous detection with both electrical and optical signals, thus confirming unambiguously that the modulation of electrical current corresponded to a molecular translocation event.^[42] Similarly to longer DNA strands, guanosine triphosphate gave unusual, giant current pulses during translocation with a \sim 0.5-1.2 ms duration.^[41] Interestingly, transient current increases were observed regardless of the charge polarity of the dye (**Figure 2b**).^[42] As for ssDNA, the current spikes were attributed to an increase in electroosmotic current due to an augmented charge imbalance inside the SWNT when the charged dye molecule entered the nanochannel.^[42] The dwell times of fluorescent dye translocation events in 20- μ m-long SWNT were much longer than for similar-size guanosine triphosphate (\sim 100-700 ms) and comparable to those of ssDNA oligonucleotides.

3.3.2. Controversies and Open Questions

Demonstrating and detecting translocation of small analytes as well as larger, biologically-relevant molecules through a SWNT is a critical breakthrough. It opens opportunities toward the application of these channels for single-molecule sensing and biomolecule detection based on the Coulter principle, as well as biophysics tools for studying biomolecular motion in confined geometries.^[9] For the advancement of these fields, it is of paramount importance to 1) fully understand the ionic current signature associated with a given translocation event; and 2) extract relevant kinetic or physical parameters from the transient current modulation. The electrical signals obtained so far with μm -long SWNTs are quite different from those of protein nanochannels and other solid-state nanopores.^[59] Instead of the conventional current blockades,^[59] large current increases were observed for both polyvalent ssDNA oligomers and mono-to-trivalent small analytes when they passed through the core of CNT channels. To our knowledge, no previous study showed current spikes during monovalent analyte translocation, whereas, in some conditions, DNA strands were reported to produce transient current increases in solid state nanopores^[34] and inorganic nanotubes.^[35] The origin of these current spikes in μm -long SWNTs may be connected with the unique structural, electrical and chemical properties of these graphitic pores, and further elucidation is needed to employ the transient current signal in quantitative analysis. The differences in the oligonucleotide translocation signal (spikes versus blockades) in μm -long SWNTs^[40] when compared to that in either μm -long MWNTs^[40] or in ultrashort SWNTs (within CNT-lipid hybrids)^[50, 51] is striking. Understanding the precise origin of these differences may provide insight on which channel geometrical properties dictate the dominant molecular transport mode (electrophoresis versus electroosmosis) and the current modulation associated with the molecular motion.

4. Conclusions, Challenges, and Future Directions

As highlighted above, the advent of fluidic experiments with individual SWNTs has led to surprising observations that challenge our understanding of transport of inorganic electrolytes, small molecules, as well as larger oligonucleotides. Moreover, in several instances, several SWNT platforms gave differing outcomes, and it remains unclear if variations in platform design are partially responsible for the reported discrepancies. In order to resolve these apparent controversies and open questions, it is vital to continue developing single-SWNT nanofluidic platforms with enhanced control and functionalities, and to perform rigorous tests

to demonstrate that transport is indeed through a single CNT pore. With these advanced devices, researchers can fully elucidate the interplay between the structural, geometrical, and electronic characteristics of CNTs, and how these properties dictate their unique molecular and ionic transport behavior.

The ideal nanofluidic device should allow flexibility in tuning the properties of each component comprising the platform, which includes the insulating material chemistry, pore diameter and length, functionalization at the CNT rim, defect density and charge of the graphitic wall, etc. Moreover, the platform should be highly reproducible, robust, and easy to regenerate to enable many experiments in a wide range of conditions with the same nanochannel or with many devices with identical isolated nanochannels.

In particular, building SWNT devices with prescribed diameter and chirality is required to unravel the effect of CNT electronic properties on the fluid motion as well as the dependence of transport rates on pore size. Hosting isolated SWNTs with length varying from sub- μm up to mm within a single platform design could decouple effects of CNT length from the influence of extrinsic (and less controllable) platform design factors. This would provide crucial insight on the fundamentally different ionic and molecular transport behavior in ultrashort CNT-lipid hybrid and μm -long SWNT solid-state devices and, thus, help establish a unified picture for transport inside a CNT.

Coupling independent detection techniques with current-pulse sensing in the same experiment is expected to be greatly beneficial to interpret unambiguously the electric signal and for advanced single-molecule detection schemes. Integrated gate electrodes in the CNT fluidic platform could be key to controlling molecule translocation speed^[30] and help reveal the underlying mechanism for unusually large ion conductances and their anomalous dependence on electrolyte concentration.

Full elucidation of fluid flow in CNTs requires convergence between results from individual SWNT devices and CNT membranes. In several instances, water flow enhancement and electrolyte conductances measured with CNT membranes differ markedly from those measured with single CNT devices (see **Table 1** and **2**). A platform design that could selectively isolate a prescribed number of conductive CNT channels could offer a tool to pinpoint the origin of reported discrepancies. While so-far researchers have limited the studies to electric field driven transport, the ability to apply other driving forces such as a pressure gradient, would facilitate a deeper understanding of CNT nanofluidic phenomena and the interplay of different transport mode.

In addition to the experimental effort, synergistic multiscale simulations of experimentally relevant geometries and conditions are critical to unravel the underlying mechanistic origin of observed phenomena. The benefit of this two-sided approach is expected to be particularly far reaching for CNTs because these nanochannels have simple geometry, structural features, and chemistry, all of which facilitate accurate modeling. While there is already a large body of literature on simulations of fluids in CNTs, these calculations often use force fields that have been parameterized to reproduce bulk fluid properties rather than the actual behavior under nanoconfinement.^[7] These simulations also often neglect polarization effects, which may influence fluid flow in CNTs.^[7] Comparison with single-CNT experimental studies may help establish if these models are reliable to describe fluid flow in nanoconfined environments.

To summarize, the reviewed research poses a list of exciting questions regarding the physics of reported nanofluidic phenomena and will certainly spawn numerous experimental and theoretical follow-up studies. The anomalous fluidic behavior of nanometer-wide SWNT channels offers opportunities for enhanced functionality and novel combinations of properties, which promises to open a fascinating new chapter in the nanofluidics field. Specifically, the large ionic conductance could boost the efficiency of energy storage and harvesting devices, while rapid proton transport could be exploited for fuel cells both in self-powered miniaturized systems or larger scale devices.^[5] In the near future, it may be possible to build nanotube-based circuits with selective functional gates wherein fluidics and electronics are coupled.^[30] With such advanced device architecture, molecular and ionic transport could be manipulated with vastly enhanced control for applications in sensing, separation, detection, and therapeutic delivery.

Acknowledgements

This work was enabled by financial support from a Laboratory Directed Research and Development project at Lawrence Livermore National Laboratory (LDRD# 13-ERD-030) and from the UC Lab Fees Research Program (UCOP Grant ID # 236772). S. Guo, E. Meshot, and F. Fornasiero would like to acknowledge partial financial support of the Chemical and Biological Technologies Department of the Defense Threat Reduction Agency (DTRA-CB) via grant BA12PHM123 in the “Dynamic Multifunctional Materials for a Second Skin D[MS]²” program. Work at LLNL was performed under the auspices of the US Department of Energy under contract DE-AC52-07NA27344. Work at the Molecular Foundry was

supported by the Office of Science, Office of Basic Energy Sciences, of the US Department of Energy under contract DE-AC02-05CH11231.

Received: ((will be filled in by the editorial staff))

Revised: ((will be filled in by the editorial staff))

Published online: ((will be filled in by the editorial staff))

- [1] R. B. Schoch, J. Y. Han, P. Renaud, *Rev. Mod. Phys.* **2008**, *80*, 839.
- [2] L. Bocquet, E. Charlaix, *Chem. Soc. Rev.* **2010**, *39*, 1073.
- [3] J. K. Holt, *Adv. Mater.* **2009**, *21*, 1.
- [4] A. Noy, H. G. Park, F. Fornasiero, J. K. Holt, C. P. Grigoropoulos, O. Bakajin, *Nano Today* **2007**, *2*, 22.
- [5] H. G. Park, Y. Jung, *Chem. Soc. Rev.* **2014**, *43*, 565.
- [6] M. F. L. De Volder, S. H. Tawfick, R. H. Baughman, A. J. Hart, *Science* **2013**, *339*, 535.
- [7] A. Alexiadis, S. Kassinos, *Chemical Reviews* **2008**, *108*, 5014.
- [8] L. Sun, R. M. Crooks, *J Am Chem Soc* **2000**, *122*, 12340.
- [9] Z. S. Siwy, M. Davenport, *Nat. Nanotechnol.* **2010**, *5*, 174.
- [10] F. Fornasiero, H. G. Park, J. K. Holt, M. Stadermann, C. P. Grigoropoulos, A. Noy, O. Bakajin, *Proc. Natl. Acad. Sci. U. S. A.* **2008**, *105*, 17250.
- [11] R. Garcia-Fandino, M. S. P. Sansom, *Proc. Natl. Acad. Sci. U. S. A.* **2012**, *109*, 6939.
- [12] M. Majumder, N. Chopra, B. J. Hinds, *J. Am. Chem. Soc.* **2005**, *127*, 9062; J. Wu, X. Zhan, B. J. Hinds, *Chemical Communications* **2012**, *48*, 7979.
- [13] J. K. Holt, H. G. Park, Y. M. Wang, M. Stadermann, A. B. Artyukhin, C. P. Grigoropoulos, A. Noy, O. Bakajin, *Science* **2006**, *312*, 1034.
- [14] A. I. Skoulidas, D. M. Ackerman, J. K. Johnson, D. S. Sholl, *Phys. Rev. Lett.* **2002**, *89*, 4.
- [15] M. Majumder, N. Chopra, R. Andrews, B. J. Hinds, *Nature* **2005**, *438*, 44.
- [16] S. Joseph, N. R. Aluru, *Nano Lett.* **2008**, *8*, 452.
- [17] C. Dellago, M. M. Naor, G. Hummer, *Phys. Rev. Lett.* **2003**, *90*, 4.
- [18] G. Hummer, *Mol. Phys.* **2007**, *105*, 201.
- [19] G. Hummer, J. C. Rasaiah, J. P. Noworyta, *Nature* **2001**, *414*, 188.
- [20] A. Kalra, S. Garde, G. Hummer, *Proc. Natl. Acad. Sci. U. S. A.* **2003**, *100*, 10175.
- [21] K. Falk, F. Sedlmeier, L. Joly, R. R. Netz, L. Bocquet, *Nano Lett.* **2010**, *10*, 4067.
- [22] T. A. Pascal, W. A. Goddard, Y. Jung, *Proc. Natl. Acad. Sci. U. S. A.* **2011**, *108*, 11794.
- [23] K. Koga, G. T. Gao, H. Tanaka, X. C. Zeng, *Nature* **2001**, *412*, 802.
- [24] H. J. Gao, Y. Kong, D. X. Cui, C. S. Ozkan, *Nano Lett.* **2003**, *3*, 471.
- [25] I. C. Yeh, G. Hummer, *Proc. Natl. Acad. Sci. U. S. A.* **2004**, *101*, 12177; U. Zimmerli, P. Koumoutsakos, *Biophys. J.* **2008**, *94*, 2546.
- [26] J. Wu, K. S. Paudel, C. Strasinger, D. Hammell, A. L. Stinchcomb, B. J. Hinds, *Proc. Natl. Acad. Sci. U. S. A.* **2010**, *107*, 11698.
- [27] X. Pan, Z. Fan, W. Chen, Y. Ding, H. Luo, X. Bao, *Nature Materials* **2007**, *6*, 507.
- [28] B. Corry, *Energy Environ. Sci.* **2011**, *4*, 751; W.-F. Chan, H.-y. Chen, A. Surapathi, M. G. Taylor, X. Hao, E. Marand, J. K. Johnson, *Acs Nano* **2013**, *7*, 5308.
- [29] G. A. Pilgrim, J. W. Leadbetter, F. Qiu, A. J. Siitonen, S. M. Pilgrim, T. D. Krauss, *Nano Lett.* **2014**, *14*, 1728.

- [30] S. G. Lemay, *Angew. Chem.-Int. Edit.* **2010**, *49*, 7627.
- [31] Z. W. Ulissi, S. Shimizu, C. Y. Lee, M. S. Strano, *Journal of Physical Chemistry Letters* **2011**, *2*, 2892.
- [32] T. Ito, L. Sun, R. R. Henriquez, R. M. Crooks, *Acc. Chem. Res.* **2004**, *37*, 937.
- [33] S. Howorka, Z. Siwy, *Chem. Soc. Rev.* **2009**, *38*, 2360.
- [34] H. Chang, F. Kosari, G. Andreadakis, M. A. Alam, G. Vasmatzis, R. Bashir, *Nano Lett.* **2004**, *4*, 1551; S. W. Kowalczyk, C. Dekker, *Nano Lett.* **2012**, *12*, 4159; R. M. M. Smeets, U. F. Keyser, D. Krapf, M. Y. Wu, N. H. Dekker, C. Dekker, *Nano Lett.* **2006**, *6*, 89; D. M. Vlassarev, J. A. Golovchenko, *Biophys. J.* **2012**, *103*, 352.
- [35] R. Fan, R. Karnik, M. Yue, D. Y. Li, A. Majumdar, P. D. Yang, *Nano Lett.* **2005**, *5*, 1633.
- [36] K. E. Venta, M. B. Zanjani, X. C. Ye, G. Danda, C. B. Murray, J. R. Lukes, M. Drndic, *Nano Lett.* **2014**, *14*, 5358.
- [37] R. R. Henriquez, T. Ito, L. Sun, R. M. Crooks, *Analyst* **2004**, *129*, 478.
- [38] T. Ito, L. Sun, R. M. Crooks, *Anal. Chem.* **2003**, *75*, 2399.
- [39] R. R. Henriquez, T. Ito, L. Sun, R. M. Crooks, *Analyst* **2004**, *129*, 478.
- [40] H. T. Liu, J. He, J. Y. Tang, H. Liu, P. Pang, D. Cao, P. Krstic, S. Joseph, S. Lindsay, C. Nuckolls, *Science* **2010**, *327*, 64.
- [41] J. He, H. Liu, P. Pang, D. Cao, S. Lindsay, *Journal of Physics-Condensed Matter* **2010**, *22*.
- [42] W. S. Song, P. Pang, J. He, S. Lindsay, *Acs Nano* **2013**, *7*, 689.
- [43] D. Cao, P. Pang, J. He, T. Luo, J. H. Park, P. Krstic, C. Nuckolls, J. Tang, S. Lindsay, *Acs Nano* **2011**, *5*, 3113.
- [44] P. Pang, J. He, J. H. Park, P. S. Krstic, S. Lindsay, *Acs Nano* **2011**, *5*, 7277.
- [45] D. Cao, P. Pang, H. Liu, J. He, S. M. Lindsay, *Nanotechnol.* **2012**, *23*.
- [46] X. C. Qin, Q. Z. Yuan, Y. P. Zhao, S. B. Xie, Z. F. Liu, *Nano Lett.* **2011**, *11*, 2173.
- [47] W. Choi, C. Y. Lee, M. H. Ham, S. Shimizu, M. S. Strano, *J. Am. Chem. Soc.*, *133*, 203.
- [48] W. Choi, Z. W. Ulissi, S. F. E. Shimizu, D. O. Bellisario, M. D. Ellison, M. S. Strano, *Nature Communications* **2013**, *4*.
- [49] C. Y. Lee, W. Choi, J.-H. Han, M. S. Strano, *Science* **2010**, *329*, 1320.
- [50] L. Liu, C. Yang, K. Zhao, J. Li, H.-C. Wu, *Nat Commun* **2013**, *4*.
- [51] J. Geng, K. Kim, J. Zhang, A. Escalada, R. Tunuguntla, L. R. Comolli, F. I. Allen, A. V. Shnyrova, K. R. Cho, D. Munoz, Y. M. Wang, C. P. Grigoropoulos, C. M. Ajo-Franklin, V. A. Frolov, A. Noy, *Nature* **2014**, *514*, 612.
- [52] S. Guo, S. F. Buchsbaum, E. R. Meshot, M. W. Davenport, Z. Siwy, F. Fornasiero, *Biophys. J.* **2015**, *108*, 175a.
- [53] J. A. Thomas, A. J. H. McGaughey, *Phys. Rev. Lett.* **2009**, *102*.
- [54] J. A. Thomas, A. J. H. McGaughey, *Nano Lett.* **2008**, *8*, 2788.
- [55] J. H. Walther, K. Ritos, E. R. Cruz-Chu, C. M. Megaridis, P. Koumoutsakos, *Nano Lett.* **2013**, *13*, 1910.
- [56] S. K. Kannam, B. D. Todd, J. S. Hansen, P. J. Davis, *The Journal of Chemical Physics* **2013**, *138*.
- [57] J. Wu, K. Gerstandt, H. B. Zhang, J. Liu, B. J. Hinds, *Nat Nanotechnol* **2012**, *7*, 133.
- [58] J. H. Park, J. He, B. Gyrfas, S. Lindsay, P. S. Krstic, *Nanotechnol.* **2012**, *23*.
- [59] B. M. Venkatesan, R. Bashir, *Nat. Nanotechnol.*, *6*, 615.
- [60] M. Majumder, N. Chopra, B. J. Hinds, *Acs Nano* **2011**, *5*, 3867.
- [61] P. Krishnakumar, P. B. Tiwari, S. Staples, T. Luo, Y. Darici, J. He, S. M. Lindsay, *Nanotechnol.* **2012**, *23*.

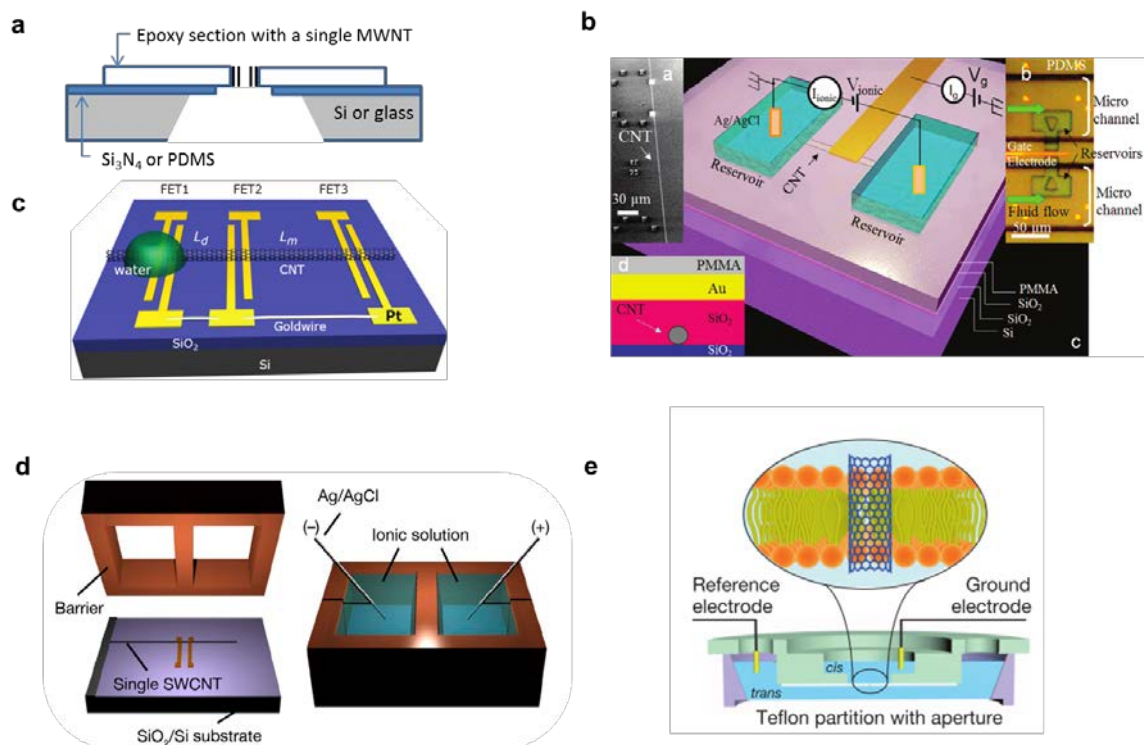


Figure 1. Schematic representations of platforms for single CNT nanofluidics. a) Vertically aligned MWNT embedded in an epoxy film mounted either on a Si/Si₃N₄ (200 nm)^[8] or on a glass/PDMS (500 μm) support with a micron sized hole.^[38] b) Combined SWNT horizontal fluidic channel and CNT-FET. Reproduced with permission.^[44] Copyright 2013, American Chemical Society. c) Array of FETs built on an individual SWNT to measure water transport rates. Reproduced with permission.^[46] Copyright 2011, American Chemical Society. d) Ultralong SWNT flow channel connecting two reservoirs defined by photolithography in an epoxy structure. Reproduced with permission.^[49] Copyright 2010, Science. e) A hybrid platform with an ultrashort SWNT crossing a lipid bilayer membrane. Reproduced with permission.^[51] Copyright 2014, Nature Publishing Group.

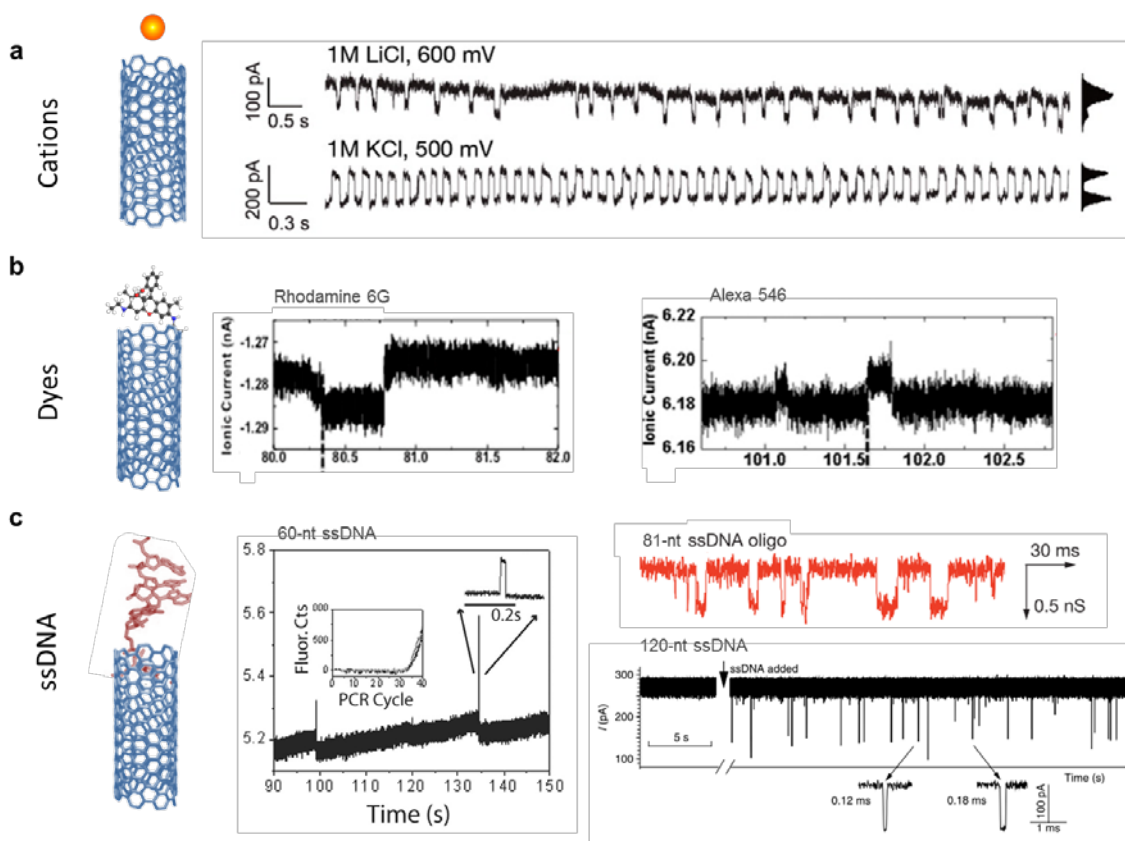


Figure 2. Examples of ionic current modulations generated by a single molecule translocation. a) Ionic current blockades induced by Li^+ and K^+ cations showing coherence resonance with sustained oscillations. Reproduced with permission.^[49] Copyright 2010, Science. b) Transient ionic current increase generated by the transit of small dye molecules through the core of a μm -long SWNT. Reproduced with permission.^[42] Copyright 2013 American Chemical Society. c) Oligonucleotide translocation through a SWNT in three different platforms: left) current spikes observed in a solid state device similar to that represented in Figure 1.b;^[40] right) current blockades recorded with hybrid platforms made of a lipid bilayer membrane with self-inserted (top)^[51] or injected (bottom)^[50] ultrashort SWNT. Reproduced with permission.^[40, 50, 51] Copyright 2010, Science Copyright 2013, Nature Publishing Group and Copyright 2014, Nature Publishing Group.

Table 1. Water transport in CNTs: slip lengths and flow rate enhancement factors with respect to Hagen-Poiseuille law predicted by molecular dynamics simulations, and experimentally measured with multi-pore CNT membranes and single-CNT platforms. For a comprehensive summary, see a recent review by Kannam et al. ^[56]

Reference	Barrier material	Two-state blockades	CNT type	Electrical property ^{a)}	CNT length	CNT diameter [nm]	Water velocity [mm s ⁻¹]	Slip length [nm]	Enhancement factor ^{b)}					
<i>Qin</i> ^[46]	None (Control experiment: photoresist)	N/A Not tested for molecule translocation	SWNT/ CVD	S Small bandgap	140 & 280 μm	0.81 – 1.59	0.046 – 0.928 ^{c)}	8 – 53 ^{d)}	51 – 882 ^{d)}					
						0.81	0.928	53	882					
						0.87	0.671	44.6	662					
						0.98	0.312	29.3	354					
						1.10	0.366	56.6	580					
						1.42	0.073	13.5	103					
						1.52	0.049	8.4	59					
						1.59	0.046	7.9	51					
						Multi-pore membranes								
						<i>Holt</i> ^[13]	Si ₃ N ₄	N/A	DWNT/ Vertically aligned CVD	N/A	2 – 3 μm	1.3 – 2.0	2.3 – 15 ^{f)}	140 – 1400
<i>Majumder</i> ^[15, 60]	Polystyrene	N/A	MWNT/ Vertically aligned CVD	M	34 – 126 μm	7.0	95 – 439 ^{f)}	39000 – 68000	44000 – 76000					
Simulations														
<i>Thomas</i> ^[53]	None	N/A	SWNT	M	75 & 150 nm	0.81 – 1.39	1 – 7 x10 ^{-3 g)}	N/A	150 – 6500					
						0.83								
						0.96								
						1.10								
						1.25								
						1.39								
						1.66								

(Continue on next page)

Table 1. Water transport in CNTs: slip lengths and flow rate enhancement factors predicted by molecular dynamics simulation (*continuation*).

Reference	Barrier material	Two-state blockades	CNT Type	Electrical property	CNT length	CNT diameter [nm]	Water velocity [mm s ⁻¹]	Slip length [nm]	Enhancement factor
Thomas ^[54]	None	N/A	SWNT	M	12 – 80 nm	1.66 – 4.99	3 – 14 x10 ^{3 g)}	30 – 105	47 – 433
						1.66		107	
						2.22		62.2	
						2.77		46.6	
						3.33		39.5	
						4.44		34.0	
4.99	32.8								
Joseph ^[16]	None	N/A	SWNT	M	Infinitely long	2.2	~200 x10 ^{3 h)}	564 ⁱ⁾	2052
Walther ^[55]	Hydrophilic	N/A	DWNT	M	1.4 nm – 2 μm 3 nm 6 nm 12 nm 30 nm 2 μm	2.0	N/A	<63	<253
Falk ^[21]	None	N/A	SWNT	S, M	Infinitely long	0.68-20.4	~10 – 45 x10 ^{3 h)}	80 – >500	32 – >4000 ⁱ⁾
						1		~500	~4000
						7		~120	~138
Kannam ^[56]	None	N/A	SWNT	M	7.37-2.45 nm	1.62 – 6.5	~2 – 30 x10 ^{3 h)}	75 – 180	90 – 870 ⁱ⁾
						1.62		180 ⁱ⁾	870 ⁱ⁾
						1.90		160	680
						2.16		140	525
						2.72		120	350
						3.26		110	260
						3.80		100	210
						4.34		100	180
						4.88		95	160
						6.50		75	90

a) M=metallic, S=semiconductive; b) the enhancement factor is defined as the ratio Q/Q_{HP} , where Q is the measured water flow rate and Q_{HP} the flow rate predicted by Hagen-Poiseuille law; c) spontaneous wetting; d) calculations use CNT inner diameter and bulk water viscosity; e) calculations use full CNT diameter and modified water viscosity; f) applied pressure = 1 bar; g) applied pressure gradient = $0.5-3 \times 10^{14}$ and $2-10 \times 10^{14}$ Pa/m^[54]; h) applied external accelerations = 2×10^{-3} nm/ps²,^[16] $\sim 10^{-4}$ nm/ps²,^[21] $0.2-2 \times 10^{-4}$ nm/ps²^[56]; i) enhancement factor, E , and slip length, L_s , are related by $E=1+4L_s/R_{CNT}$, where is R_{CNT} the CNT radius; j) approximate values extracted from Figure 5 of Reference^[56]

Table 2. Ionic transport in a single CNT.

Group	Platform ^{a)}	Two-state blockades	Barrier material	CNT type	Electrical property ^{b)}	Length	Diameter [nm]	G in a single CNT at 1M KCl (nS) ^{c)}	n in $G \sim C_{KCl}^n$	I-V ^{d)}
<i>Lindsay</i> ^[40]	SS-H	No, spikes with ssDNA	PMMA (750 nm)	SWNT/ CVD	M	2 μ m	1.7 – 4.2 1.7 2.0 4.2	~4.5 – 27 6.8 26.8 6.3	0.3-0.4	L (-0.5 \div 0.5 V)
		No current pulses for SWNTs with $G < 2$ nS			S		0.9 – 3.4 0.9 1.1 1.3 1.8 3.4	-0.025 – 2.5 2.5 0.2 0.9 0.2 <0.025		
<i>Lindsay</i> ^[44]	SS-H	N/A Not tested for molecule translocation	SiO ₂ (20 nm) + PMMA (900 nm)	SWNT/ CVD	M, S	20 μ m	0.5 – 4.0	44 (-0.5 – 10.5 at 1 mM KCl)	0.37 (unspecified wide range)	L (-0.8 \div 0.8 V)
<i>Crooks</i> ^[32, 38]	SS-V	Yes PS-NP ^{e)}	Epoxy	MWNT/ CVD	M	~1 μ m	80 – 130	150 – 200	N/A	L (-0.5 \div 0.5V)
<i>Strano</i> ^[48]	SS-H	Yes cations	Epoxy (1.5 mm)	SWNT/ CVD	M, S	1000 μ m	0.9 – 2	~0.1 – 10 (at 3M KCl)	N/A	N/A
<i>Strano</i> ^[49]	SS-H	Yes cations	Epoxy (1.5 mm)	SWNT/ CVD	M, S	500 μ m	1.3 – 2.3	-0.6 (at 1M NaCl)	N/A	L (0 \div 1.0 V)
<i>Wu</i> ^[50]	hybrid	Yes ssDNA	Lipid bilayer	SWNT acid cut	M	5 – 10 nm	0.5 – 2.0	~60 – 100	N/A	L (-0.15 \div 0.15 V)
					S		1 – 2	~3 – 24		L (-0.2 \div 0.2 V)
					S		<1	~0.1 – 2		NL (-0.2 \div 0.2 V)
<i>Noy</i> ^[51]	hybrid	Yes ssDNA	Lipid bilayer	SWNT sonication cut	N/A	5 – 15 nm	1.5 \pm 0.21	~0.6	1	L (N/A)

(Continue on next page)

Table 2. Ionic transport in a single CNT (*continuation*).

Group	Platform	Two-state blockades	Barrier material	CNT type	Electrical property	Length	Diameter [nm]	G in a single CNT at 1M KCl (nS)	n in $G \sim C_{KCl}^n$	I-V
Multi-pore membranes										
<i>Lindsay</i> ^[61]	SS-V	N/A	Parylene	MWNT/ Vertically aligned CVD	M	42 μ m	7	~0.17	1	L (-2 \div 2 V)
<i>Hinds</i> ^[57]	SS-V	N/A	Epoxy	SWNT/ CVD Shear mixed with epoxy	1/3 M 2/3 S	5 μ m	0.9 \pm 0.2	~0.0007	1	L (-0.6 \div 0.6V)

^{a)} SS=solid state, H=horizontal, V=vertical; ^{b)} M=metallic, S=semiconductive; ^{c)} G=conductance; ^{d)} voltage window during I-V testing in parenthesis, L=linear, NL=non-linear I-V curve; ^{e)} PS-NP = polystyrene nanoparticles

Table 3. Single molecule translocation in a single CNT.

Group	Platform ^{a)}	Barrier material	Two-state blockades	CNT type	Electrical property ^{b)}	Length	Diameter [nm]	Molecule	Signal	Amplitude ^{c)} [pA]	Dwell time ^{c)} [ms]
<i>Lindsay</i> ^[40, 41]	SS-H	PMMA ^[40] (750nm)	No, spikes with nucleotides	SWNT/ CVD	SWNT with $G > 2$ nS, mostly M	2 μ m	0.9 – 4.2	60-nt ssDNA ^[40]	Spikes	100 – 1000 (0.4-0.5 V)	~10
		120-nt ssDNA ^[40]			Spikes			50 – 200 (0.5 V)	~100		
		PMMA ^[41] (800nm)			N/A		1.6 average	Guanosine triphosphate ^[41]	Spikes	1000 – 2000 (0.7 V)	0.86±0.15
<i>Lindsay</i> ^[42]	SS-H	SiO ₂ (20 nm) + PMMA (800 nm)	No, spikes with dyes	SWNT/ CVD	N/A	20 μ m	2±0.8	Alexa 546	Spikes	14±4 (0.4 – 0.5 V)	160±90
								Rhodamine 6G		9 – 10 (0.4 – 0.5 V)	260 – 730
<i>Strano</i> ^[49]	SS-H	Epoxy	Yes cations	SWNT/ CVD	M/S	500 μ m	1.3 – 2.3	Na ⁺	Blockades	120 – 420 (0.6 V)	~ 10
								Li ⁺		7.5 – 145 (0.6 V)	20 – 200
								K ⁺		52 – 323 (0.5 V)	10 – 110

(Continue on next page)

Table 3. Single molecule translocation in a single CNT (*continuation*).

Group	Platform ^{a)}	Barrier material	Two-state blockades	CNT type	Electrical property ^{b)}	Length	Diameter [nm]	Molecule	Signal	Amplitude ^{c)} [pA]	Dwell time ^{c)} [ms]
<i>Strano</i> ^[48]	SS-H	Epoxy	Yes cations	SWNT/ CVD	M, S	1000 μ m	0.9 – 2	Na ⁺ , Li ⁺ , K ⁺ , Cs ⁺	Blockades	10 – 800 ^{d)}	0.02 – 600 ^{d)}
					M		0.94	60 – 90 ^{e)}		0 – 20 ^{e)}	
					M		1.27	20 – 40		70 – 170	
					M		1.37	10 – 40		10 – 500	
					S		1.39	10 – 30		0 – 400	
					M		1.40	15 – 35		0 – 300	
					M		1.44	20 – 50		0 – 90	
					S		1.48	30 – 70		0 – 160	
					S		1.49	45 – 120		0 – 60	
					S		1.50	25 – 100		0 – 150	
					S		1.54	30 – 90		0 – 600	
					S		1.57	100 – 500		0 – 45	
					M		1.58	200 – 800		0 – 200	
					S		1.63	100 – 400		0 – 300	
					M		1.67	60 – 120		0 – 15	
					M		1.7	100 – 200		0 – 30	
					S		1.74	50 – 70		10 – 30	
S	1.77	10 – 70	0 – 90								
S	1.85	30 – 45	25 – 150								
S	1.92	10 – 40	0 – 350								
M	2.01	40 – 80	0 – 10								
<i>Wu</i> ^[50]	hybrid	Lipid bilayer	Yes ssDNA	SWNT/ acid cut	S	5 – 10 nm	1 – 2	120-nt ssDNA	Blockades	50 – 200 (30 mV)	~0.1 – 100
<i>Noy</i> ^[51]	hybrid	Lipid bilayer	Yes ssDNA	SWNT/ sonication cut	N/A	5 – 15 nm	1.5 \pm 0.21	81-nt ssDNA	Blockades	20 – 200 (-50 mV)	53 ^{f)}

^{a)} SS=solid state, H=horizontal; ^{b)} M=metallic, S=semiconductive; ^{c)} typical applied voltages in the range 0.1-1.0 V for SS devices and 0.01-0.1 V for hybrid platforms; ^{d)} varying with CNT diameter and cation type; ^{e)} approximate values at 1.0 V extracted from Figures S5-S7 of Reference ^[48]; ^{f)} center of a Gaussian distribution of dwell times.

The table of contents

Fluidic measurements through the interior of an individual SWNT promise to enable a quantum-leap advancement of the nanofluidic field. Experiments with single-CNT fluidic platforms reveal an unusual, yet exciting transport behavior for water, ion, and single molecules confined in a CNT. These unique transport properties offer opportunities for enhanced functionality in future nanofluidic devices for applications in sensing, separation, detection, and therapeutic delivery.

Keyword CNT nanofluidics

S. Guo, E. R. Meshot, T. Kuykendall, S. Cabrini, F. Fornasiero*

Nanofluidic Transport Through Isolated Carbon Nanotube Channels: Advances, Controversies, and Challenges

ToC figure

